Curvature-tuned electronic properties of bilayer graphene in an effective four-dimensional spacetime

Marco Cariglia,[1,2,3] Roberto Giambò,[4] and Andrea Perali[2,5]
[1]*Departamento de Física, Universidade Federal de Ouro Preto, 35400-000 Ouro Preto MG, Brazil*
[2]*School of Pharmacy, Physics Unit, Università di Camerino, 62032-Camerino, Italy*
[3]*Dipartimento di Fisica e Astronomia, Università degli studi di Padova, via F. Marzolo 8, 35131 Padova, Italy*
[4]*School of Science and Technology, Mathematics Division, University of Camerino, 62032-Camerino, Italy*
[5]*INFN, Sezione di Perugia, 06123-Perugia, Italy*
(Received 26 November 2016; revised manuscript received 21 May 2017; published 23 June 2017)

We show that in AB stacked bilayer graphene low-energy excitations around the semimetallic points are described by massless, four-dimensional Dirac fermions. There is an effective reconstruction of the four-dimensional spacetime, including in particular the dimension perpendicular to the sheet, that arises dynamically from the physical graphene sheet and the interactions experienced by the carriers. The effective spacetime is the Eisenhart-Duval lift of the dynamics experienced by Galilei invariant Lévy-Leblond spin-$\frac{1}{2}$ particles near the Dirac points. We find that changing the intrinsic curvature of the bilayer sheet induces a change in the energy level of the electronic bands, switching from a conducting regime for negative curvature to an insulating one when curvature is positive. In particular, curving graphene bilayers allow opening or closing the energy gap between conduction and valence bands, a key effect for electronic devices. Thus, using curvature as a tunable parameter opens the way for the beginning of curvatronics in bilayer graphene.

DOI: 10.1103/PhysRevB.95.245426

I. INTRODUCTION

The investigation of condensed matter systems, particularly in the nanometric regime and from the point of view of new materials with tunable electronic properties, has assumed a primary role in physics to understand many-body systems from first principles and to devise new technological applications. In the last few years, a series of advances, both experimental and theoretical, have made evident that new materials in the quantum regime present a range of phenomena that are well understood using concepts of relativistic particle physics, until recently thought to be removed from practical applications. Nowadays, related activities are relevant topics in the physics community, and as an important example we cite that of studying massless and massive Dirac fermions in graphene. Here, the state of the art is that of using the formalism of three-dimensional (3D) quantum field theory on curved spacetime to describe electronic properties of the material, where the effective curved geometry is originated by properties of the structure such as interaction with a substrate, topological defects such as disclinations and dislocations, or ripples [1–9]. Distortions of the bilayer graphene lattice, induced for instance by an applied curvature, have been considered as a mechanism to tune and bend the quasiparticle energy dipersion because they generate new phonons interacting with conduction electrons in a nontrivial way. Corresponding electronic and polaronic properties associated to these effects have been discussed extensively in Refs. [10–13]. In the study of superconductors, which also represent condensed matter systems with high potential for technological breakthroughs, there is some experimental evidence for fractal geometries in cuprates [14–17], however, no experiment in a curved geometry setting, while a recent theoretical work investigates the effects of curvature on the superconducting pairing in the presence of spin-orbit coupling, predicting nontrivial spin-triplet textures of the pairs [18]. In the case of carbon nanotubes, effects of curvature on the electronic structure and transport have been studied [19–21].

In this work, we extend to bilayer graphene the relativistic approach and the methods of effective geometry for the massless Dirac fermion of monolayer graphene, generalizing it by showing that the geometry can include extra dimensions that are related to an effective reconstruction of the full ambient spacetime. We show that there is an effective four-dimensional (4D) spacetime, in general curved, where solutions of the massless Dirac equation are in correspondence to low-energy solutions of the original tight-binding model, in the continuum limit. This approach shows explicitly that even for bilayer graphene there are massless excitations, which is of interest on its own, and moreover is particularly powerful since properties of the system can be inferred by known geometrical methods. For example, we show in a simple way how the local two-dimensional (2D) curvature affects the local energy density and the electronic structure. This is a kinematical effect that arises from the bound motion in a curved space, and is different in nature from the electrical gating effect, that is due to interaction with external fields. This provides a new mechanism to generate a gap in the energy levels.

The outline of the paper is the following. In Sec. II we begin showing that the quasifree excitations in AB stacked bilayer graphene obey, in the low-energy limit, the Galilei invariant Lévy-Leblond equations for a spin-$\frac{1}{2}$ particle. In Sec. III we demonstrate that these solutions can be lifted to solutions of the massless Dirac equation in 4D Minkowski space. Next, we generalize this geometrical construction first in Sec. IV by addition of a transverse, constant magnetic field, and then in Sec. V, considering a curved 2D sheet of bilayer graphene and discussing its consequences on the electronic properties. In particular, the energy band gap is evaluated as a function of the curvature radius. Positive (resp. negative) curvature of the bilayer graphene is associated with insulating (resp. metallic)

behavior of the system. Possible applications of *curvatronics* are finally outlined in the concluding Sec. VI.

II. LOW-ENERGY SOLUTIONS OF THE EFFECTIVE HAMILTONIAN IN *AB* BILAYER GRAPHENE

The electronic band structure of graphite was studied in 1947 using a tight-binding model by Wallace [22]. Nowadays, we know that for graphene there exist pairs of Dirac points K and K' at the corners of the first Brillouin zone in momentum space, such that excitations with momentum sufficiently close to K or K' display a linear dispersion relation, and we call these points "valleys". The distinct honeycomb lattice of graphene decomposes into two inequivalent A and B triangular lattices and these excitations are described by a massless, covariant, continuum theory for two degrees of freedom in two dimensions, obtained from the Dirac equation in the plane. The recent reference [23] contains technical details and a literature overview.

We start from the low-energy limit tight-binding model Hamiltonian of AB stacked bilayer graphene close to the K or K' points

$$H_{K,K'} = \begin{pmatrix} 0 & \hbar v_F \kappa & 0 & \gamma \\ \hbar v_F \bar{\kappa} & 0 & 0 & 0 \\ 0 & 0 & 0 & \hbar v_F \kappa \\ \gamma & 0 & \hbar v_F \bar{\kappa} & 0 \end{pmatrix}, \tag{1}$$

where $\kappa = \tau k_x + i k_y$ is the wave number of the excitation. $\tau = \pm 1$ denotes the Hamiltonian relative to the K or K' point, $\gamma \sim 0.4$ eV is the hopping parameter between A_1 and B_2 sites, while $v_F \sim 10^6$ ms^{-1} is the Fermi velocity in a graphene monolayer close to the Dirac points.

The eigenvectors associated with the eigenvalue equation $H\lambda = E\lambda$ are

$$\lambda_1 = 1, \quad \lambda_2 = \frac{\hbar v_F \bar{\kappa}}{E}, \quad \lambda_3 = \sigma \frac{\hbar v_F \kappa}{E}, \quad \lambda_4 = \sigma, \tag{2}$$

where $\bar{\kappa}$ is the complex conjugate of κ, λ_j $(j = 1, \ldots, 4)$ are the components of the eigenvectors, and the energy E satisfies the consistency condition

$$E^2 - |\hbar v_F \kappa|^2 = \sigma \gamma E, \quad \sigma = \pm 1 . \tag{3}$$

For each value of τ there are four solutions: for $\sigma = \pm 1$ there are two eigenvalues of the energy. The spectrum is valley degenerate, while the spinors (2) are not. We group the eigenvalues in two families:

$$E_i^{(\pm)} = \pm \left[(-1)^i \frac{\gamma}{2} + \sqrt{\frac{\gamma^2}{4} + |\hbar v_F \kappa|^2} \right], \quad i = 1,2. \tag{4}$$

The $E_1^{(\pm)}$ bands touch at $|\kappa| = 0$ and make bilayer graphene a semimetal, while the $E_2^{(\pm)}$ bands are separated by a distance 2γ.

For low values of κ, all bands grow quadratically, which indicates nonrelativistic behavior. In fact, as we show in the rest of this section the low-energy excitations satisfy the Lévy-Leblond equations: nonrelativistic, Galilei invariant equations for a spin-$\frac{1}{2}$ particle of mass m [24]. These were written in 1967 as a nonrelativistic limit of the Dirac equation, and proved that the $g = 2$ Landé factor for the electron is not a relativistic property. In our case, the mass is proportional to the hopping parameter γ.

We expand the solutions to leading order in the dimensionless parameter $\epsilon = \frac{\hbar v_F |\kappa|}{\gamma}$. For the $E_1^{(\pm)}$ bands

$$\lambda_2 = \pm \frac{\gamma}{\hbar v_F \kappa} + O(\epsilon), \quad \lambda_3 = \pm \sigma \frac{\gamma}{\hbar v_F \bar{\kappa}} + O(\epsilon), \tag{5}$$

while for the $E_2^{(\pm)}$ bands

$$\lambda_2 = \pm \frac{\hbar v_F \bar{\kappa}}{\gamma} + O(\epsilon^3), \quad \lambda_3 = \pm \sigma \frac{\hbar v_F \kappa}{\gamma} + O(\epsilon^3). \tag{6}$$

The Lévy-Leblond equations are written in terms of two time-dependent spinors $\chi_1(t)$, $\chi_2(t)$ with two components:

$$i\hbar\, \partial_t \chi_2 + i\hbar v_F D \chi_1 = 0, \tag{7}$$

$$D\chi_2 - i \frac{2m v_F}{\hbar} \chi_1 = 0, \tag{8}$$

where $D = i\sigma^j k_j$ is the two-dimensional Dirac operator in phase space and the σ^j are the Pauli matrices in the standard basis. We replaced the speed of light c in the original work with the relevant speed $v_F \sim \frac{c}{300}$ here.

Solutions of (7) and (8) can be obtained from (5) and (6). For $E = E_1^{(\pm)}$ and $\tau = 1$,

$$\chi_1(t) = e^{\mp i \frac{|\hbar v_F \kappa|^2}{\hbar \gamma} t} (\lambda_1, \sigma \lambda_4)^T, \tag{9}$$

$$\chi_2(t) = e^{\mp i \frac{|\hbar v_F \kappa|^2}{\hbar \gamma} t} (\lambda_2, \sigma \lambda_3)^T, \tag{10}$$

where the mass is given by $m = \pm \frac{\gamma}{2 v_F^2}$. For $E = E_2^{(\pm)}$ the solution is obtained swapping $\chi_1 \leftrightarrow \chi_2$ above, while for $\tau = -1$ the solutions are generated by the substitution $\kappa \to -\bar{\kappa}$. Let us recall that λ_1 and λ_4 are related to components of the wave function on two stacked sites of type A-B where up-down hopping is allowed, while the λ_2, λ_3 components are associated to sites which are not directly overlapping and for which hopping is negligible.

III. MASSLESS 4D FERMIONS

The massive Lévy-Leblond equations can be obtained from the massless Dirac equation in a spacetime with two extra dimensions [25–28]. The construction is based on the Eisenhart-Duval lift of dynamics, which was first discussed by Eisenhart [29] in the first half of the previous century, and then independently rediscovered by Duval and collaborators [30,31]. The lift establishes a correspondence between classical, nonrelativistic motions in the presence of a scalar and vector potential and null geodesics in a higher-dimensional spacetime, and extends to quantum mechanics relating the nonrelativistic Schrödinger equation with the higher-dimensional Klein-Gordon equation, and the Lévy-Leblond with the Dirac equation. The technique has been successfully used for several applications as, for example, higher derivative systems [32] and nonrelativistic holography [33–35], inspired by previous results in holography [36]; see [37] for a review of the associated geometry.

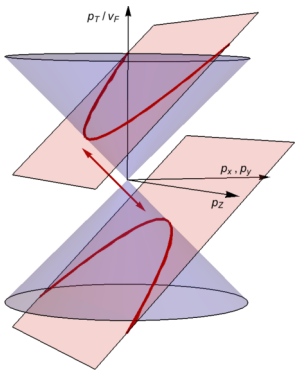

FIG. 1. The 4D massless Dirac cone $p_x^2 + p_y^2 + 2p_u p_v$ is cut by the plane $p_v = m v_F$. The result is the nonrelativistic parabola $E = \frac{1}{2m}(p_x^2 + p_y^2)$, where $E = -v_F p_u$. In our notation $p_Z = \frac{1}{\sqrt{2}}(p_u + p_v)$, $p_T = \frac{v_F}{\sqrt{2}}(p_u - p_v)$.

As an example, the trajectory of a classical free point particle with unit mass moving on a plane can be lifted, using Eisenhart-Duval correspondence, to a null geodesic of the Minkowski metric in 4D written in double-null coordinates u and v:

$$g_{\mu\nu} dx^\mu dx^\nu = dx^2 + dy^2 + 2\,du\,dv. \tag{11}$$

The 4D variable u corresponds, in a standard identification, with $v_F t$, where t is the time coordinate in the 2D dynamics. For a massless particle the null cone is $g^{\mu\nu} p_\mu p_\nu = 0$, where p_μ are the momenta. Since the metric does not depend on v, then the condition $p_v = m v_F$ can be imposed. The intersection of this plane with the null cone yields the nonrelativistic parabolic dispersion relation, as shown in Fig. 1. 4D gamma matrices Γ^μ satisfy the algebra $\{\Gamma^\mu, \Gamma^\nu\} = 2g^{\mu\nu}$. Spinors in 4D have four components, spinors in 2D have two. We adopt a decomposition of Dirac matrices suitable for the null form of the metric:

$$\Gamma^+ = \begin{pmatrix} 0 & \mathbb{I} \\ 0 & 0 \end{pmatrix}, \quad \Gamma^- = 2\begin{pmatrix} 0 & 0 \\ \mathbb{I} & 0 \end{pmatrix}, \quad \Gamma^i = \begin{pmatrix} \sigma_i & 0 \\ 0 & -\sigma_i \end{pmatrix}.$$

The 4D Dirac operator decomposes as

$$\hat{D} = \begin{pmatrix} D & \partial_u \\ 2\partial_v & -D \end{pmatrix}, \tag{12}$$

where $D = \sigma^i \partial_i$ is the 2D Dirac operator. The matrix above is not symmetric under the exchange of the u, v coordinates. The factor of 2 has been chosen in order to recover the Lévy-Leblond equations, as discussed below. Solutions of the massless Dirac equation in 4D, $\hat{D}\,\hat{\Psi} = 0$, are compatible with the lightlike projection

$$\partial_v \hat{\Psi} = i \frac{m v_F}{\hbar} \hat{\Psi} \tag{13}$$

since the Minkowski metric is independent of v. Upon using this projection, one immediately sees that (12) induces the Lévy-Leblond equations (7) and (8). Therefore, we reach the important conclusion that the 4D spinor

$$\hat{\Psi} = e^{i \frac{m v_F}{\hbar} v} \begin{pmatrix} \chi_1(u) \\ \chi_2(u) \end{pmatrix} \tag{14}$$

satisfies the massless four-dimensional Dirac equation in flat space. The four possible spinors are in one-to-one correspondence with the low-energy solutions of the tight-binding model of bilayer graphene close to the Dirac points.

To conclude this section, we define 4D variables Z, T using $u = \frac{Z + v_F T}{\sqrt{2}}$, $v = \frac{Z - v_F T}{\sqrt{2}}$, such that $2\,du\,dv = dZ^2 - v_F^2 dT^2$. To lowest order in ϵ, the T, z dependence of our solutions is of the kind $e^{i \frac{\gamma}{\hbar v_F} \frac{Z - v_F T}{2\sqrt{2}}}$ from which we infer a wavelength along the Z direction with value $4\sqrt{2}\pi \frac{\hbar v_F}{\gamma} = 29$ nm, large compared to the real thickness of the bilayer. Therefore, the effective description adopted here, where an effective flat space appears that is infinitely extended in all directions, is compatible with the real bilayer electronic structure: the wave function $\hat{\Psi}$ is not able to resolve the real finite thickness.

IV. TRANSVERSE MAGNETIC FIELD

The results obtained so far are not limited to the special case of free bilayer graphene. The only constraint is that the Eisenhart-Duval lift cannot describe external fields that depend on the v direction: a dependence on the 2D time variable t is allowed but not one on Z. So, the case of an electric field transverse to the plane, and hence to the bilayer graphene, cannot be treated in this framework.

In this section, we show that our results continue being valid in the presence of a constant, transverse magnetic field $\vec{B} = B\,\hat{e}_Z$. The tight-binding Hamiltonian is obtained from (1) with the substitution

$$\hbar k \to \pi = -i\hbar\left(\tau \partial_x + i \partial_y + \frac{eBx}{\hbar}\right), \tag{15}$$

arising from the standard definition of covariant momentum $\vec{p} - e\vec{A}$, and in a gauge where the only nonzero component of the gauge potential is $A_y = Bx$. This Hamiltonian applies if the lattice spacing is much smaller than the magnetic length $l_B = \sqrt{\frac{\hbar}{eB}}$. We look for solutions to the eigenvalue equation in the form $\lambda = e^{ik_y y}\varphi(x)$. In the rest of the section, we will identify the operator π with its reduction on the φ type of spinors, i.e., we will write $\pi = -i\hbar(\tau \partial_x - k_y + \frac{eBx}{\hbar})$. The problem reduces to the quantum harmonic oscillator since the rescaled operators $a = \frac{1}{\sqrt{2\hbar eB}}\pi = -\frac{i}{\sqrt{2}}(\tau \partial_\xi + \xi)$, and similarly for $a^\dagger$ satisfy the Heisenberg algebra. Here, $\xi = \frac{x}{l_B} - k_y l_B$ is a dimensionless quantity. We employ the ansatz $\varphi_1 = \psi_n(\xi)$, where ψ_n is the nth level normalized eigenfunction of the quantum mechanical harmonic oscillator. For nonzero energy we find

$$\tilde{E}_{1,2} = \pm\left(\frac{2n + 1 + \tilde{\gamma}^2 \pm \sqrt{\tilde{\gamma}^4 + (4n+2)\tilde{\gamma}^2 + 1}}{2}\right)^{\frac{1}{2}},$$

where $\tilde{E} = \frac{E}{\sqrt{2\hbar eB} v_F}$ and similarly for γ, which agrees with the formulas reported in the literature; see, e.g., [23, Eq. (2.49)]. In particular for the $n = 0$ level there is no gap opening: this effect is the same in the case of the pseudomagnetic fields arising from strain, when present. In the next section, we will show that instead intrinsic curvature of the surface can open a gap: this underlies the difference between the effects of strain

and those of curvature. The remaining spinor components are

$$\varphi_2 = \frac{\sqrt{n+1}}{\tilde{E}}\psi_{n+1}, \quad \varphi_3 = \sqrt{n}\,\frac{\tilde{E}^2-(n+1)}{\tilde{E}^2\tilde{\gamma}}\psi_{n-1}, \quad (16)$$

$$\varphi_4 = \frac{\tilde{E}^2-(n+1)}{\tilde{E}\tilde{\gamma}}\psi_n\,. \quad (17)$$

Now, we examine the low-energy limit and show that it is again described by the Lévy-Leblond equations. For $B=0$ it must be $\frac{\pi\pi^\dagger+\pi^\dagger\pi}{2} = |\hbar\kappa|^2$, while for finite B we have $\frac{\pi\pi^\dagger+\pi^\dagger\pi}{2} = 2\hbar eB(N+1/2)$, where $N=a^\dagger a$ is the number operator. Therefore, we take the limit $B\to 0$ together with $n\to+\infty$ so that $2\hbar eBv_F^2(n+1/2)\sim|\hbar v_F\kappa|^2 \ll \gamma^2$. In this limit, the Landau levels of bilayer graphene become

$$E_1^{(\pm)} \sim \pm\frac{2\hbar eBv_F^2(n+1/2)}{\gamma}, \quad E_2^{(\pm)}\sim\pm\gamma + E_1^{(\pm)}. \quad (18)$$

On the other hand, the solutions of the Lévy-Leblond equations for the $E_1^{(\pm)}$ bands are

$$\chi_1(t) = \begin{pmatrix} e^{\mp in\frac{eB}{m}t}\,\frac{\sqrt{n2\hbar eB}}{2mv_F}\psi_n \\ e^{\mp i(n+1)\frac{eB}{m}t}\,\frac{\sqrt{(n+1)2\hbar eB}}{2mv_F}\psi_n \end{pmatrix}, \quad (19)$$

$$\chi_2(t) = \left(e^{\mp i(n+1)\frac{eB}{m}t}\psi_{n+1}, e^{\mp in\frac{eB}{m}t}\psi_{n-1}\right)^T, \quad (20)$$

while for the $E_2^{(\pm)}$ bands

$$\chi_1(t) = \begin{pmatrix} e^{\mp i(n+1)\frac{eB}{m}t}\,\frac{\sqrt{(n+1)2\hbar eB}}{2mv_F}\psi_{n+1} \\ e^{\mp in\frac{eB}{m}t}\,\frac{\sqrt{n2\hbar eB}}{2mv_F}\psi_{n-1} \end{pmatrix}, \quad (21)$$

$$\chi_2(t) = \left(e^{\mp in\frac{eB}{m}t}\psi_n, e^{\mp i(n+1)\frac{eB}{m}t}\psi_n\right)^T. \quad (22)$$

In the former case for low-energy $\binom{\chi_1(t)}{\chi_2(t)} \sim \frac{\sqrt{(n+\frac{1}{2})2\hbar eB}}{2mv_F}e^{\mp i\frac{E_1^{(\pm)}}{\hbar\gamma}t}(\lambda_1,\sigma\lambda_4,\lambda_2,\sigma\lambda_3)^T$, and in the latter $\binom{\chi_1(t)}{\chi_2(t)} \sim e^{\mp i\frac{(E_2^{(\pm)}\mp\gamma)}{\hbar\gamma}t}(\lambda_2,\sigma\lambda_3,\lambda_1,\sigma\lambda_4)^T$, which are the same relations found in the free case. The mass of the low-energy excitations is still given by $m=\pm\frac{\gamma}{2v_F^2}$. Therefore, in this section we have demonstrated that the Lévy-Leblond equations describe the low-energy limit of the electronic spectrum, split in Landau levels, of bilayer graphene systems in the presence of an external magnetic field perpendicular to the layers.

V. EXTENSION TO CURVED SPACE: CURVATRONICS

To extend the example of the classical free point particle examined above, let us consider a generic 2D Riemannian space $\mathcal{M}$ with metric

$$g = g_{ij}(x)dx^i dx^j,$$

and the classical theory of a particle of mass m and electric charge e on $\mathcal{M}$, interacting with a scalar potential V and an electromagnetic field with vector potential A_i, both possibly depending on position and time. In this case, the Hamiltonian is given by

$$H = \frac{g^{ij}}{2m}(p_i - eA_i)(p_j - eA_j) + V.$$

Then, Eisenhart-Duval lift is given by the 4D Lorentzian metric

$$ds^2 = g_{ij}\,dq^i dq^j + \frac{2e}{mv_F}A_i dq^i du + 2\,du\,dv - \frac{2V}{mv_F^2}du^2,$$

where $q^i=(x,y)$, $A_i(q,u)$, and $V(q,u)$ are the vector and scalar potential. Note that the external potentials do not depend on the transverse v direction, as pointed out above. To see that this is correct, one can calculate the geodesic Hamiltonian from the metric above, obtaining

$$\mathcal{H} = \frac{g^{ij}}{2m}\left(p_i - \frac{e\,p_v}{mv_F}A_i\right)\left(p_j - \frac{e\,p_v}{mv_F}A_j\right) + \frac{p_u p_v}{m} + \frac{V}{m^2v_F^2}p_v^2\,.$$

Setting $p_v = mv_F$, and $\mathcal{H}=0$ for null geodesics we obtain the condition

$$v_F\,p_u = -H\,. \quad (23)$$

If we define a new variable t by $u=v_F\,t$, then the equation above says that H, the generator of time translations for the original dynamical system in 2D, can be identified with minus the momentum along the t direction, which justifies identifying the variable t with the time parameter in 2D.

As a further generalization, g can be considered as a time-dependent 2D metric, which implies that g_{ij} are also functions of (q,u). Explicitly time-dependent systems have been recently discussed in [38], where it has been shown that the formalism of the Eisenhart lift is compatible with the time dependence, both classically and quantum mechanically. To generalize the projection of the 4D Dirac operator (12) described above to this case, the curvature of the Riemannian manifold $\mathcal{M}$ must be taken into account, and this can be accomplished using the covariant spinorial derivatives defined in [28], retrieving the operator, with a slight correction with respect to [28, Eq. (4.11)]

$$\hat{D} = \begin{pmatrix} \frac{i}{\hbar}\,\Pi & \partial_u + i\,\frac{V}{\hbar v_F} \\ 2i\,\frac{mv_F}{\hbar} & -\frac{i}{\hbar}\,\Pi \end{pmatrix}. \quad (24)$$

Here, $\Pi = \sigma^j\Pi_j$ and $\Pi_j = -i\hbar\nabla_j - eA_j$ is the U(1) covariant momentum including the spin connection, and we used the projection (13). It can be seen from (24) that the massless, 4D Dirac equation $\hat{D}\hat{\Psi}=0$ induces the curved version of the Lévy-Leblond equations (7) and (8) when $\hat{\Psi}$ is of the form (14). The equations obtained automatically include the presence of a scalar and vector potential, and of a curved 2D metric g_{ij}. In particular, they incorporate the results above discussed for magnetic fields. Therefore, nonrelativistic Lévy-Leblond fermions, arising in the continuum limit of the tight-binding theory in bilayer graphene in presence of potentials independent of the variable v, are described by a massless Dirac equation in the effective 4D geometry. Bilayer sheets with constant curvature are represented in Fig. 2. In the literature on monolayer graphene it is known that, using a covariant version of the Dirac equation, one should consider effects of strain of the atomic lattice that produce pseudomagnetic effective fields [39–42]. It is also known that the effects of strain are important, as they induce strong effective magnetic fields. The effective magnetic fields arising

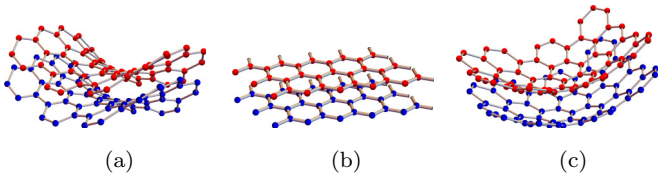

FIG. 2. Structures of bilayered graphene for different values of the 2D curvature. (a) $R < 0$ corresponds to hyperbolic geometry, (b) $R = 0$ to the flat graphene bilayer, (c) $R > 0$ to spherical geometry.

from strain modify the energy spectrum by inducing Landau levels. In particular, there always exists a zero Landau level and no gap in the energy spectrum can be opened in this way. As we are going to show next, our geometrical analysis shows that the local curvature of the sheet can be used to tune a gap opening: since this effect is different in nature from that of strain, in this work as a first step in the description of curved bilayer graphene we do not include the effects of strain. These are important and will be included in a future work. The formalism we use has the important advantage of linking directly the curvature of the 2D geometry to the energy of states. We realize the geometrical description with a locally Minkowski 4D metric, describing soft deformations of the bilayer structure that maintain the first-order structure of the hexagonal cells, without local lattice strains or compressions of the bonds within the cells. For a nontrivial g_{ij}, the energy can be considered low if at all points $\hbar^2 v_F^2 R \ll \gamma^2$, where R is the Ricci scalar of g.

From Eq. (24) one obtains the curved version of the Lévy-Leblond equations with a scalar potential. Taking two derivatives of χ_2 we obtain the Schrödinger equation

$$\left(\mathcal{E} - \frac{g^{ij}}{2m}\Pi_i \Pi_j - V + \frac{e\hbar}{2m}B - \frac{\hbar^2}{8m}R\right)\chi_2 = 0, \qquad (25)$$

where $\mathcal{E} = i\hbar\,\partial_t$. For a surface of constant radius of curvature l_R then $|R| = \frac{2}{l_R^2}$, and if the R term in (25) is smaller than γ, we obtain $l_R \gg 1.16$ nm, in agreement with requirements of smooth deformations on scales larger than the hexagonal cell. Experimental values of the energy contribution that can be measured by ARPES photoemission spectroscopy are of the order of $E_A = 10^{-3}$ eV: requiring that the curvature effects are measurable with photoemission results in the constraint $l_R \leqslant 23$ nm. This is well within the typical curvature scale of interest in graphene systems [43–45]. The scalar curvature of the surface has been discussed in the context of curved monolayer graphene in [46], where it has been associated to an effective pseudomagnetic field.

The case $V = 0$, $B = 0$ can be studied in terms of the eigenvalues $\mathfrak{p}$ of the spinorial momentum operator Π, proportional to the Dirac operator: then $\mathcal{E} = \frac{\mathfrak{p}^2}{2m}$. For example, in the case of a sphere of radius l_R the eigenvalues are known [47], and the quantized energy is

$$\mathcal{E} = \pm n^2 \frac{\hbar^2 v_F^2}{l_R^2 \gamma} \quad n \in \mathbb{Z}^*, \qquad (26)$$

where no zero modes of the Dirac operator exist on the sphere. The expression is valid for $\frac{l_R}{n} > \frac{\hbar v_F}{\gamma} = 1.16$ nm, and describes

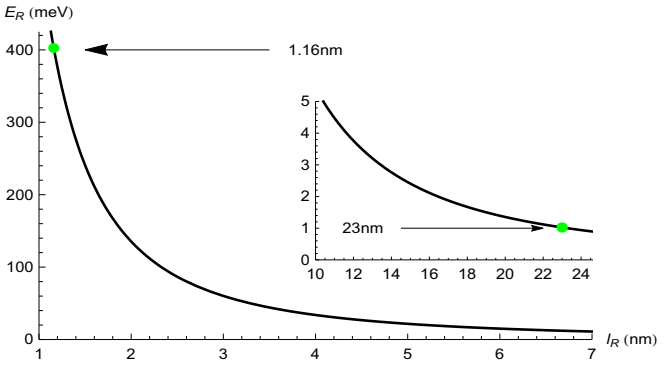

FIG. 3. Energy band gap between conduction and valence bands E_R as a function of the (constant) curvature radius l_R. The arrows indicate the validity range of our approach.

the two touching energy bands, as well as the departure from γ of the nontouching bands.

Our results imply that for a positive curvature surface, the energy of + bands will be shifted higher, while the energy of the − bands will be shifted lower, due to the sign change in the effective mass. Therefore, the shifted E_1 bands will make the bilayer graphene a semiconductor with a tunable band gap proportional to R. In Fig. 3, the energy band gap $E_R = E_1^{(+)} - E_1^{(-)}$ is plotted as a function of the curvature radius l_R, for positive constant curvature. Considering, for instance, the range 3 nm $< l_R <$ 4 nm, Fig. 3 shows that the band gap is in the range $E_R \simeq$ 40–60 meV, already enough to suppress thermal broadening and thermal excitations across the bands at or below room temperature. Band-gap opening in bilayer graphene of energies of the order shown in Fig. 3 have been obtained by electric field gating as measured in Ref. [52], following the earlier prediction of Ref. [48]. On the other hand, negative curvature makes the material a conductor to leading order. Negative curvature can be applied to 2D semiconducting systems, as bilayer graphene with a band gap induced by an external potential, to reduce or close the band gap, increasing progressively their metallic behavior.

Modifications of the electronic band dispersions in graphene systems, including opening of an energy band gap, can be induced by lattice strain perturbations. Recent experimental investigation for bilayer graphene is reported in [2]. The effects of strains are quite different if applied to monolayer or bilayer graphene. In the case of monolayer graphene, the band-gap opening is difficult to achieve: only acting with strain along precise directions above a threshold deformation of 20%, the band gap starts to appear, as obtained by a tight-binding approach in Ref. [49]. On the contrary, and most relevant for this work, bilayer graphene has more degrees of freedom to which strain deformations can be applied, compared to monolayer graphene: strain can act in the lateral directions symmetric among the layers, asymmetric among the layers, and in the direction perpendicular to the bilayer. By a tight-binding approach and linear elasticity theory, Ref. [50] demonstrates that perpendicular strain opens a gap at the $K = 0$ point, as in our case with positive curvature, because the inequivalence of A and B atoms of the sublattices is enhanced by the strain (and by the curvature). Also, the perpendicular

strain has a threshold around 25% of deformation and a deformation of 30% can generate a sizable band gap of 125 meV. Interestingly, an asymmetric strain of the two layers of the graphene bilayer generates a band gap with a much smaller deformation and without a threshold: already at 5% of deformation a band gap of 10 meV opens. The opening of a band gap by asymmetric strain in bilayer graphene has been confirmed by *ab initio* calculations of the band structure [51]. We expect therefore that curvature of bilayer graphene mixes strains in the different directions and will be most effective in opening a band gap between the conduction and the valence bands in comparison with uniaxial strain usually considered in monolayer graphene.

The reader might wonder what is the physical reason behind the opening of a gap due to curvature, and if there is any relation with the previously known phenomenon of tunable gap opening by electrical gating. As remarked in [52], a crucial reason why electrical gating opens a gap is that it breaks the inversion symmetry of bilayer graphene. We have investigated this issue and found that curvature does not break the inversion symmetry. Rather, while electrical gating is a dynamical effect, i.e., due to the interaction with an external field, the gap opening that we discuss in this work is kinematical in nature. The R term present in the Schrödinger equation (25) arises directly from the term

$$[\nabla_i, \nabla_j] = \tfrac{1}{4} R_{ijlm} \Gamma^{lm} \tag{27}$$

that expresses the noncommutation of (spinorial) covariant derivatives in curved space. In other words the gap arises from the properties of propagation of fields in the curved space, that are required by covariance and by consistency with the bound motion.

In the literature for monolayer graphene, curvature is in connection with two opposite effects on electronic states: in an earlier work using a continuum model positive curvature was found to repel charges, and negative curvature to attract them [53], while more recent work that uses the Dirac equation on a curved background found that positive curvature conical defects are associated to an increase in the DOS, and vice versa for negative curvature [1,54]. On the one hand, the results of [53] should provide a refinement, smaller and in the opposite direction, of analyses based on the connectivity of single sites. On the other hand, it is unclear if the results of [1] are due to the singularity or to the curvature: conical defects are singular points with zero intrinsic curvature, and the effects described are very localized, disappearing a few lattice constants away from the defect. Our approach describes long-range curvature and therefore is complementary to that of [54]. In fact, it is a second-order effect: the energies in [1] are of the order of $E_{loc} = \frac{\hbar v_F}{l_R}$, while those in our model, using the value of m in (25), are $E_{\text{geom}} = \frac{\hbar^2 v_F^2}{2\gamma l_R^2}$. In fact, these are the two allowed combinations of parameters with which one can build an energy. Then, our earlier requirement of low energy $\hbar^2 v_F^2 R \ll \gamma^2$ implies $E_{\text{geom}} \ll E_{\text{loc}}$.

These results are important in the development of graphene-based curvatronics as they give a powerful tool to describe the local effect of curvature on electronic states in (25). They are also important in the fundamental understanding of bilayer graphene and can be applied to other 2D materials with massive quasiparticles.

VI. CONCLUSIONS

We have shown that the low-energy limit of the continuum tight-binding model for AB stacked bilayer graphene is given by the Galilei invariant Lévy-Leblond equations. Using the Eisenhart-Duval lift we proved that the low-energy excitations satisfy the massless Dirac equation in an effective 4D Lorentzian geometry that reconstructs the full space. The parabolic dispersion relations of bilayer graphene look conical from a 4D perspective. We presented detailed evidence for free bilayer graphene and bilayer graphene with a transverse, constant magnetic field. Application to a curved 2D sheet yields a simple and powerful relationship between the Ricci curvature of the surface and the local energy of the excitations, that arises from kinematical effects. The theory models the effect of long-range curvature and is complementary, but with opposite behavior, to the theory of curvature generated by local defects. Our results open the way to curvatronics for tuning the electronic properties of graphene systems by local, smooth deformations, in such a way to allow and control a continuous crossover from metallic to semiconducting behavior and vice versa. Our geometrical approach can be also applied to other ultrathin materials and tested on naturally curved systems, as fullerenes with their number of carbon atoms controlling the curvature, including fullerenes with concentric onionlike structures having a spherical bilayer of carbon atoms generating a band gap [55]. Geometrical effects are also relevant for metamaterials with interesting topological properties, in which positive or negative curvature may induce very different effects and generate topological transitions [56].

ACKNOWLEDGMENTS

We would like to thank L. Covaci, L. Dell'Anna, M. Doria, C. Duval, P. Horváthy, A. Marcelli, D. Neilson, and M. Zarenia for useful discussions. M.C. would like to thank the Physics Unit in Camerino and the Physics Department in Padova for hospitality, and acknowledges CNPq support from Project No. 205029/2014-0 and FAPEMIG support from Project No. APQ-02164-14. A.P. acknowledges financial support from the University of Camerino under the project FAR "Control and enhancement of superconductivity by engineering materials at the nanoscale". We acknowledge the collaboration within the MultiSuper International Network (http://www.multisuper.org) for exchange of ideas and suggestions.

[1] M. A. H. Vozmediano, M. I. Katsnelson, and F. Guinea, Gauge fields in graphene, Phys. Rep. **496**, 109 (2010).

[2] W. Yan *et al.*, Strain and curvature induced evolution of electronic band structures in twisted graphene bilayer, Nat. Commun. **4**, 2159 (2013).

[3] S. Ulstrup, J. C. Johannsen, F. Cilento, J. A. Miwa, A. Crepaldi, M. Zacchigna, C. Cacho, R. Chapman, E. Springate, S. Mammadov, F. Fromm, C. Raidel, T. Seyller, F. Parmigiani, M. Grioni, P. D. C. King, and P. Hofmann, Ultrafast Dynamics of Massive Dirac Fermions in Bilayer Graphene, Phys. Rev. Lett. **112**, 257401 (2014).

[4] O. Boada, A. Celi, J. I. Latorre, and M. Lewenstein, Dirac equation for cold atoms in artificial curved spacetimes, New J. Phys. **13**, 035002 (2011).

[5] N. Szpak, A Sheet of Graphene Quantum Field in a Discrete Curved Space, in *Relativity and Gravitation*, edited by J. Bičák and T. Ledvinka (Springer, Berlin, 2014), p. 583.

[6] V. Atanasov and A. Saxena, Electronic properties of corrugated graphene, the Heisenberg principle and wormhole geometry in solid state, J. Phys.: Condens. Matter **23**, 175301 (2011).

[7] A. Iorio, Graphene: QFT in curved spacetimes close to experiments, J. Phys.: Conf. Ser. **442**, 012056 (2013).

[8] A. Cortijo and M. A. Zubkov, Emergent gravity in the cubic tight-binding model of Weyl semimetal in the presence of elastic deformations, Ann. Phys. (NY) **366**, 45 (2016).

[9] C. G. Beneventano, P. Giacconi, E. M. Santangelo, and R. Soldati, Planar QED at finite temperature and density: Hall conductivity, Berrys phases and minimal conductivity of graphene, J. Phys. A: Math. Gen. **42**, 275401 (2009).

[10] Z. Li, L. Covaci, and F. Marsiglio, Impact of Dresselhaus versus Rashba spin-orbit coupling on the Holstein polaron, Phys. Rev. B **85**, 205112 (2012).

[11] Z. Li, C. J. Chandler, and F. Marsiglio, Perturbation theory of the mass enhancement for a polaron coupled to acoustic phonons, Phys. Rev. B **83**, 045104 (2011).

[12] Z. Li and J. P. Carbotte, Conductivity of Dirac fermions with phonon-induced topological crossover, Phys. Rev. B **88**, 195133 (2013).

[13] Z. Li and J. P. Carbotte, Electron-phonon correlations on spin texture of gapped helical Dirac fermions, Eur. Phys. J. B **88**, 87 (2015).

[14] H. Büttner and A. Blumen, Possible explanation for the superconducting 240-K phase in the YBaCuO system, Nature (London) **329**, 700 (1987).

[15] M. Fratini, N. Poccia, A. Ricci, G. Campi, M. Burghammer, G. Aeppli, and A. Bianconi, Scale-free structural organization of oxygen interstitials in La_2CuO_{4+y}, Nature (London) **466**, 841 (2010).

[16] J. M. Tranquada, H. Woo, T. G. Perring, H. Goka, G. D. Gu, G. Xu, M. Fujita, and K. Yamada, Quantum magnetic excitations from stripes in copper-oxide superconductors, Nature (London) **429**, 534 (2004).

[17] N. Poccia, A. Ricci, and A. Bianconi, Fractal structure favoring superconductivity at high temperatures in a stack of membranes near a strain quantum critical point, J. Supercond. Nov. Magn. **24**, 1195 (2011).

[18] Z.-J. Ying, M. Cuoco, C. Ortix, and P. Gentile, Tuning pairing amplitude and spin-triplet texture by curving superconducting nanostructures, arXiv:1704.00578.

[19] A. Kleiner and S. Eggert, Curvature, hybridization, and STM images of carbon nanotubes, Phys. Rev. B **64**, 113402 (2001).

[20] C. L. Kane and E. J. Mele, Size, Shape, and Low Energy Electronic Structure of Carbon Nanotubes, Phys. Rev. Lett. **78**, 1932 (1997).

[21] K. Falk, F. Sedlmeier, L. Joly, R. R. Netz, and L. Bocquet, Molecular origin of fast water transport in carbon nanotube membranes: Superlubricity versus curvature dependent friction, Nano Lett. **10**, 4067 (2010).

[22] P. R. Wallace, The band theory of graphite, Phys. Rev. **71**, 622 (1947).

[23] M. Zarenia, Confined states in mono-and Bi-layer graphene nanostructures, Ph.D. Thesis, Universiteit Antwerpen, 2013.

[24] J. M. Lévy-Leblond, Nonrelativistic particles and Wave Equations, Commun. Math. Phys. **6**, 286 (1967).

[25] C. Duval, The Dirac & Lévy-Leblond Equations and Geometric Quantization, in *Differential Geometric Methods in Mathematical Physics*, edited by P. L. García and A. Pérez-Rendon (Springer, Berlin, 1987), p. 205.

[26] C. Duval, P. A. Horváthy, and L. Palla, Spinor vortices in nonrelativistic Chern-Simons theory, Phys. Rev. D **52**, 4700 (1995).

[27] C. Duval, P. A. Horváthy, and L. Palla, Spinors in nonrelativistic Chern-Simons electrodynamics, Ann. Phys. (NY) **249**, 265 (1996).

[28] M. Cariglia, Hidden symmetries of Eisenhart-Duval lift metrics and the Dirac equation with flux, Phys. Rev. D **86**, 084050 (2012).

[29] L. P. Eisenhart, Dynamical trajectories and geodesics, Ann. Math. **30**, 591 (1928).

[30] C. Duval, G. Burdet, H. P. Künzle, and M. Perrin, Bargmann structures and Newton-Cartan theory, Phys. Rev. D **31**, 1841 (1985).

[31] C. Duval, G. W. Gibbons, and P. Horváthy, Celestial mechanics, conformal structures and gravitational waves, Phys. Rev. D **43**, 3907 (1991).

[32] A. Galajinsky and I. Masterov, Eisenhart lift for higher derivative systems, Phys. Lett. B **765**, 86 (2017).

[33] K. Jensen and A. Karch, Revisiting non-relativistic limits, J. High Energy Phys. **04** (2015) 155.

[34] M. Geracie, K. Prabhu, and M. M. Roberts, Curved non-relativistic spacetimes, Newtonian gravitation and massive matter, J. Math. Phys. **56**, 103505 (2015).

[35] X. Bekaert and K. Morand, Connections and dynamical trajectories in generalised Newton-Cartan gravity I. An intrinsic view, J. Math. Phys. **57**, 022507 (2016).

[36] R. A. Davison, K. Schalm, and J. Zaanen, Holographic duality and the resistivity of strange metals, Phys. Rev. B **89**, 245116 (2014).

[37] M. Cariglia, Hidden symmetries of dynamics in classical and quantum physics, Rev. Mod. Phys. **86**, 1283 (2014).

[38] M. Cariglia, C. Duval, G. W. Gibbons, and P. A. Horváthy, Eisenhart lifts and symmetries of time-dependent systems, Ann. Phys. (NY) **373**, 631 (2016).

[39] F. de Juan, A. Cortijo, and M. A. H. Vozmediano, Charge inhomogeneities due to smooth ripples in graphene sheets, Phys. Rev. B **76**, 165409 (2007).

[40] F. Guinea, M. I. Katsnelson, and A. K. Geim, Energy gaps and a zero-field quantum Hall effect in graphene by strain engineering, Nat. Phys. **6**, 30 (2010).

[41] F. de Juan, M. Sturla, and M. A. H. Vozmediano, Space Dependent Fermi Velocity in Strained Graphene, Phys. Rev. Lett. **108**, 227205 (2012).

[42] F. de Juan, J. L. Mañes, and M. A. H. Vozmediano, Gauge fields from strain in graphene, Phys. Rev. B **87**, 165131 (2013).

[43] J. C. Meyer, A. K. Geim, M. I. Katsnelson, K. S. Novoselov, T. J. Booth, and S. Roth, The structure of suspended graphene sheets, Nature (London) **446**, 60 (2007).

[44] A. H. C. Neto, F. Guinea, N. M. Peres, K. S. Novoselov, and A. K. Geim, The electronic properties of graphene, Rev. Mod. Phys. **81**, 109 (2009).

[45] M. Neek-Amal, P. Xu, J. K. Schoelz, M. L. Ackerman, S. D. Barber, P. M. Thibado, A. Sadeghi, and F. M. Peeters, Thermal mirror buckling in freestanding graphene locally controlled by scanning tunneling microscopy, Nat. Commun. **5**, 4962 (2014).

[46] E. Arias, A. R. Hernández, and C. Lewenkopf, Gauge fields in graphene with nonuniform elastic deformations: A quantum field theory approach, Phys. Rev. B **92**, 245110 (2015).

[47] J. C. Várilly, *An Introduction to Noncommutative Geometry* (European Mathematical Society, Zurich, 2006).

[48] H. Min, B. Sahu, S. K. Banerjee, and A. H. MacDonald, *Ab initio* theory of gate induced gaps in graphene bilayers, Phys. Rev. B **75**, 155115 (2007).

[49] V. M. Pereira, A. H. Castro Neto, and N. M. R. Peres, A tight-binding approach to uniaxial strain in graphene, Phys. Rev. B **80**, 045401 (2009).

[50] B. Verberck, B. Partoens, F. M. Peeters, and B. Trauzettel, Strain-induced band gaps in bilayer graphene, Phys. Rev. B **85**, 125403 (2012).

[51] S.-M. Choi, S.-H. Jhi, and Y.-W. Son, Controlling Energy Gap of Bilayer Graphene by Strain, Nano Lett. **10**, 3486 (2010).

[52] Y. Zhang, T.-T. Tang, C. Girit, Z. Hao, M. C. Martin, A. Zettl, M. F. Crommie, Y. R. Shen, and F. Wang, Direct observation of a widely tunable bandgap in bilayer graphene, Nature (London) **459**, 820 (2009).

[53] S. Azevedo, C. Furtado, and F. Moraes, Charge localization around disclinations in monolayer graphite, Phys. Status Solidi B **207**, 387 (1998).

[54] A. Cortijo and M. A. Vozmediano, Electronic properties of curved graphene sheets, Europhys. Lett. **77**, 47002 (2007).

[55] R. Pincak, V. V. Shunaev, J. Smotlacha, M. M. Slepchenkov, and O. E. Glukhova, Electronic properties of bilayer fullerene onions, arXiv:1612.01415.

[56] H. N. S. Krishnamoorthy, Z. Jacob, E. Narimanov, I. Kretzschmar, and V. M. Menon, Topological Transitions in Metamaterials, Science **336**, 205 (2012).